Pergamon

Tetrahedron 57 (2001) 4741–4751

TETRAHEDRON

Experimental and computational studies on solvent effects in reactions of peracid–aldehyde adducts

Christel Lehtinen,* Vesa Nevalainen and Gösta Brunow

Laboratory of Organic Chemistry, P.O. Box 55, FIN-00014 University of Helsinki, Finland

Received 19 October 2000; revised 13 March 2001; accepted 30 March 2001

Abstract—Solvent effects on liquid phase oxidation of aldehydes by dioxygen and *m*-chloroperbenzoic acid were studied experimentally. The main products were the corresponding carboxylic acid and a formate ester formed by Baeyer–Villiger rearrangement. In alcohol solvents (particularly methanol) substantially higher acid to formate ratios were formed than in solvents not capable of forming hydrogen bonds. Formation of both main products can be rationalised via rearrangement reactions of two epimeric peracid–aldehyde adducts, of which the interactions with methanol were studied computationally employing DFT methods at the DNPP level with the Spartan program (v5.0). The calculations indicate that structures of the adducts rearranging to give two equivalents of acid resemble the transition state of the reaction more than structures of the epimeric adducts rearranging to the acid and formate ester in 1:1 ratio. Therefore, the enhanced favor of the formation of acid in the presence of methanol can be explained in the light of Hammond's postulate.

1. Introduction

The liquid phase oxidation of aldehyde by molecular oxygen has been known for a long time. The general scheme of the free radical mechanism of oxidation of aldehyde to carboxylic acid consists of consecutive and parallel elementary stages of chain initiation, propagation, branching and termination.[1] In the final stage of reaction an aldehyde molecule and peracid, formed during the reaction, generate the adduct **1** presented in Scheme 1.[1] This further decomposes via pathways a and b to the final products.[1] A similar adduct is formed when the aldehyde is oxidised with added peracid such as *m*-CPBA.

Normally, adduct **1** rearranges by hydrogen migration to give the corresponding carboxylic acid (pathway **a**). Alternatively the carbon group can migrate and the adduct decomposes to one mole of acid and to one mole of formate (pathway **b**) (Baeyer–Villiger reaction). It is known that aromatic aldehydes,[2] α-oxygen substituted aldehydes,[3] β-lactams having a nitrogen atom at the α-position[4] and α-branched terpenic aldehydes[5] react to give the corresponding formates by oxidation with peracid but very little about the related reactions of simple aliphatic aldehydes has been published.

We recently reported the 70–80% conversion of simple aliphatic aldehydes (e.g. 2-ethylhexanal and 2-ethylbutanal) to the corresponding formates by *m*-chlorobenzoic acid treatment in dichloroethane. The α-branch in the carbon chain was found to be essential for the alkyl migration to occur.[6]

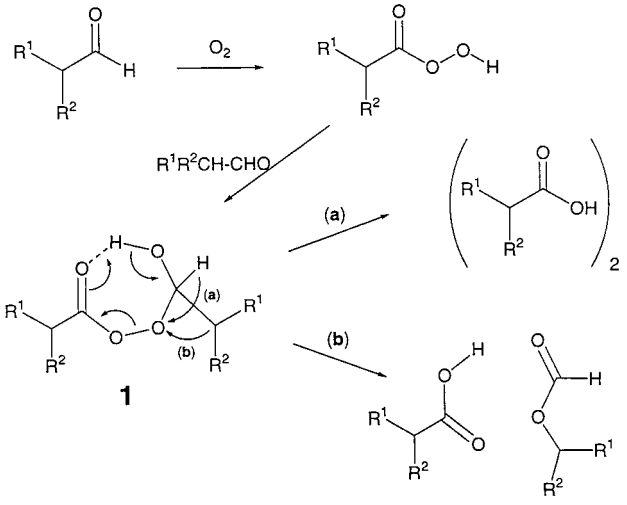

Scheme 1. Oxidation of aldehydes to the corresponding acid via reactions of peracid–aldehyde adduct **1**. Pathway **a** leads to the formation of pure acid at best whereas pathway **b** leads to a 1:1 mixture of the acid and formate.

In the present study the interest was in combining experimental work and theoretical calculations. The experimental study was aimed at the determination of solvents which can enhance the carboxylic acid formation in the reactions of **1** (i.e. favor pathway **a** over **b**, Scheme 1).

Keywords: peracid–aldehyde adducts; solvent effects; liquid phase oxidation; hydrogen bonds; computational; density function-DFT.

* Corresponding author. Tel.: +358-40-7032979; fax: +358-9-19150366; e-mail: christel.lehtinen@helsinki.fi

0040–4020/01/$ - see front matter
PII: S0040-4020(01)00397-0

In the previous comparative studies of solvent effects on the oxidation of aldehydes[7–10] only the influence of solvent on the overall reaction has been investigated. Also, the results reported in the literature are not unambiguous. In the present study we have, for the first time, been able to rationalise the observed solvent effects at the molecular level with the aid of theoretical calculations.

2. Experimental results and discussion

Effect of oxidant: The oxidation of 2-ethylhexanal, 2-ethylbutanal and 2-phenylpropanal as well as straight chain pentanal was investigated in various solvents. Molecular oxygen, *m*-CPBA and peracetic acid were used as oxidants. Peracetic acid was chosen because its structure is close to that of the peracid formed in the oxidation of a simple straight chain aldehyde. The results are presented in Tables 1 and 2.

In the O_2 oxidations two different parameters affected the conversion of aldehyde to carboxylic acid: (1) the capability of the solvent to minimise the decomposition and combination reactions of radical intermediates of aldehydes and (2) the capability of the solvent to direct the decomposition of adduct **1** either through route **a** or **b**. Only the latter effect was observed in the *m*-CPBA oxidised reactions.

When the aldehyde was oxidised with *m*-CPBA or peracetic acid, more formate was formed than in oxidations with oxygen, where the peracid for the formation of adduct **1** has to be formed in situ. The reaction was also faster and cleaner when peracid was used as oxidant. Carboxylic acid and the corresponding formate were the only products detected in oxidations with *m*-CPBA or peracetic acid, while several by-products were formed in O_2 oxidised reactions. The amount of by-products was larger when pure oxygen rather than air was used as oxidant, but the change had no effect on the formate/acid ratio of the products.

Effect of solvent: With molecular oxygen the order of reactivity of 2-ethylhexanal in the tested solvents was

Table 1. Products formed in the oxidation of 2-ethylhexanal in various solvents

Code	Solvent	Oxidant	2-ethylhexanal	Other[a] products	3-heptyl[b] formate	2-ethyl[b] hexanoic acid	Formate/acid ratio in product
1	decane	air	15.5	5.5	12.5 (15.0)	66.5 (78.5)	0.19
2	decane	*m*-CPBA	1.5	1.5	38.5 (39.0)	58.5 (59.5)	0.66
3	toluene	air	11.0	2.0	22.0 (24.5)	65.0 (73.0)	0.34
4	toluene	O_2	5.5	6.0	24.0 (25.5)	64.5 (68.0)	0.39
5	toluene	*m*-CPBA	–	–	63.5 (63.5)	36.5 (36.5)	1.77
6	oct.acid	O_2	5.5	4.0	21.0 (22.2)	69.5 (73.5)	0.30
7	oct.acid	*m*-CPBA	trace	trace	35.0 (35.0)	65.0 (65.0)	0.54
8	oct.acid	CH_3CO_3H[c]	29.0	–	25.0 (35.0)	46.0 (64.5)	0.54
9	chloroform	O_2	36.0	11.0	15.0 (27.5)	38.0 (70.3)	0.41
10	chloroform	*m*-CPBA	5.0	–	73.0 (77.0)	22.0 (23.0)	3.34
11	ethyl acet.[c]	air	5.5	14.0	9.0 (9.5)	71.5 (75.5)	0.13
12	acetic acid	air	15.5	0.5	14.5 (17.0)	69.5 (82.0)	0.21
13	$C_2H_4Cl_2$	O_2	30.0	11.5	18.0 (25.5)	40.5 (58.0)	0.44
14	$C_2H_4Cl_2$[c]	air	51.0	5.5	13.0 (26.5)	30.5 (62.0)	0.43
15	$C_2H_4Cl_2$	CH_3CO_3H[c]	45.5	2.5	34.0 (62.5)	18.0 (33.0)	1.89
16	CH_2Cl_2	*m*-CPBA	trace	trace	79.0 (79.0)	21.0 (21.0)	3.76
17	acetone[c]	O_2	2.0	17.0	3.5 (3.5)	77.5 (77.5)	0.05
18	acetone	*m*-CPBA	5.0	–	13.5 (14.0)	81.5 (86.0)	0.16
19	3-pentanone	*m*-CPBA	4.5	–	20.0 (21.0)	75.5 (78.0)	0.27
20	methanol	O_2	92	–	–	8 (100)	–
21	methanol	*m*-CPBA	5.5	–	5.5 (6.0)	89 (94.0)	0.06
22	propanol	*m*-CPBA	–	–	6.0	94.0	0.07
23	*i*-propanol	*m*-CPBA	2.7	–	5.5 (6.0)	92.5 (94.0)	0.06
24	*t*-butanol	*m*-CPBA	–	–	7.5	92.5	0.08
25	benzyl alcohol	*m*-CPBA	13.0	–	17.0 (19.5)	70.0 (81.5)	0.24
26	acetonitrile[c]	O_2	6.5	3.5	12.5 (13.5)	77.5 (83.0)	0.16
27	acetonitrile	*m*-CPBA	6.5	–	36.5 (39.0)	57.0 (61.0)	0.64
28	–	air	10.0	5.0	14.0 (15.5)	71.0 (79.0)	0.19
29	–	O_2	1.5	14.5	12.5 (13.0)	71.5(72.5)	0.18

[a] Amount of aldehyde reacted to other products than mentioned in the table, includes evaporation losses.
[b] (%) of aldehyde reacted to product.
[c] Some evaporation of mixture during the reaction. Amount of aldehyde 0.035 mol in non-solvent systems, in others 0.012 mol, 10 ml of solvent, reaction time 2h, magnetic stirring, room temperature.

Table 2. Oxidation of aldehydes with air, *m*-CPBA and O_2 as oxidants in various solvents

Aldehyde	Code	Solvent	Product distribution				Formate/acid ratio in the product
			Aldehyde	Formate	Acid	Other[a]	
2-ethyl	30	CH_2Cl_2	4	73	23	–	3.18
butanal	31	Oct.acid	1	30	69	–	0.43
	32	Oct.acid, air[b]	17	10	73	trace	0.14
2-phenyl	33	CH_2Cl_2	–	~96	~2	trace	48
propion	34	oct. acid	–	92	8	trace	11.5
aldehyde	35	toluene	trace	95	5	trace	19.0
	36	toluene[c]	trace	80.0	20.0	–	4.0
	37	benzyl alcohol	–	63.5	34.5	trace	1.84
	38	*t*-butanol	–	44.4	55.6	trace	0.80
	39	*i*-propanol	–	21.6	78.3	trace	0.27
	40	propanol	–	30.3	69.3	trace	0.44
Pentanal	41	CH_2Cl_2	–	–	100	–	–
	42	$C_2H_4Cl_2,O_2$	70.0	–	28.0	2.0	–
	43	oct.acid, O_2	~90	–	~10	–	–

Reactions were performed at room temperature, magnetic stirring, reaction time 1 to 2 h and oxidant *m*-CPBA otherwise mentioned in the table. Amount of aldehyde ~13 mmol, *m*-CPBA/aldehyde=1.2/1, 10 ml solvent. In the cases where solvent was not used, the amount of aldehyde was 36 mmol.

[a] Other products than mentioned in the table, includes evaporation losses.

[b] Air bubbling 34 ml/min.

[c] 1 equivalent (compared to aldehyde) of *t*-butanol.

the following: no solvent~acetone~ethyl acetate>toluene octanoic acid>acetonitrile>decane~acetic acid>dichloroethane>chloroform>methanol. The selectivity for acid formation in solvents deviated from the order of reactivity.

In oxidations with oxygen, the largest amounts of by-products other than formate were formed in acetone (17%, Table 1 entry 17), while the generation of by-products was most efficiently prevented in methanol (entry 20). A few side reactions occurred in acetonitrile (entry 26), octanoic (entry 11) or acetic acid (entry 12). It is noteworthy that all these solvents are able to form hydrogen bonds.

With all oxidants, the highest conversion to acid was obtained using aliphatic alcohols as solvents. Methanol, propanol and *i*-propanol were the best alcoholic solvents for 2-ethylhexanoic acid formation (entries 20–25). In benzyl alcohol *m*-CPBA as oxidant the conversion of aldehyde to acid was ~80% and to formate ~20% (entry 25) while in toluene (entries 3–5) the conversion to formate was as high as 63.5%.

A phenyl group α to the carbonyl group increases the tendency of alkyl migration in the rearrangement of adduct **1** compared to an aliphatic alkyl chain, which is reflected in the high yields of formate (entries 33 to 36).[6] The oxidation of 2-phenylpropanal was also more sensitive to solvent effects than that of 2-ethylhexanal. The highest conversion of 2-phenylpropanal to 2-phenylpropanoic acid (*m*-CPBA oxidant) was obtained in *i*-propanol, 78.3% (Table 2, entry 39). In propanol, the yield was 69.3% (entry 40) and in *t*-butanol 55.6% (entry 38).

In benzyl alcohol, reduced conversion of 2-phenylpropanal to acid was observed (34.5%, Table 2 entry 37) similarly to 2-ethylhexanal. Still, in toluene (entry 35) only 5% of the aldehyde reacted to acid. Adding 1 equivalent alcohol to the solvent (toluene) increased acid formation (entry 36) although not to the same level as in pure alcoholic solvent.

In acetone about 4% of 2-ethyhexanal reacted to give formate using O_2 as oxidant, while ~14% was formed when *m*-CPBA was used as oxidant (Table 1, entries 17 and 18). Somewhat less acid was formed in 3-pentanone (entry 19). Acetonitrile (entries 26 and 27) and decane (entries 1 and 2), behaved similarly: the ratio of formate to acid in air oxidations of 2-ethylhexanal was ~0.2 and in *m*-CPBA oxidations ~0.6–0.7.

In O_2 oxidations of 2-ethylhexanal the formate route was slightly more favored in octanoic acid (Table 1, entry 6) than in acetonitrile or decane (entries 26 and 1), whereas in *m*-CPBA oxidations the formate route was considerably less favored in octanoic acid (entry 7) than in acetonitrile or decane (entry 27 and 2). Comparison of the results for acetic and octanoic acid shows that the chain length of the solvent has little effect on to the reaction rate or path of the substrate.

Oxidations of 2-ethylhexanal in toluene, dichloroethane, dichloromethane and chloroform yielded similar ratios of formate to acid. In reactions with added peracid, the formate route dominated in chlorinated solvents by ~70–75% (entries 15 and 16) and in toluene by ~64% (entry 5). 2-Phenylpropanal was almost completely oxidised to formate in both toluene and dichloromethane as well as in octanoic acid (Table 2, entries 33–35).

Trends in the oxidation of 2-ethylbutanal were very similar to those for 2-ethylhexanal. (Table 2, entries 30–32). The formate/acid ratio of the product in octanoic acid was 0.43 (entry 31) and in dichloromethane, 3.0. Pentanal reacted in octanoic acid and dichloroethane with both oxidants molecular oxygen and *m*-CPBA only through the acid

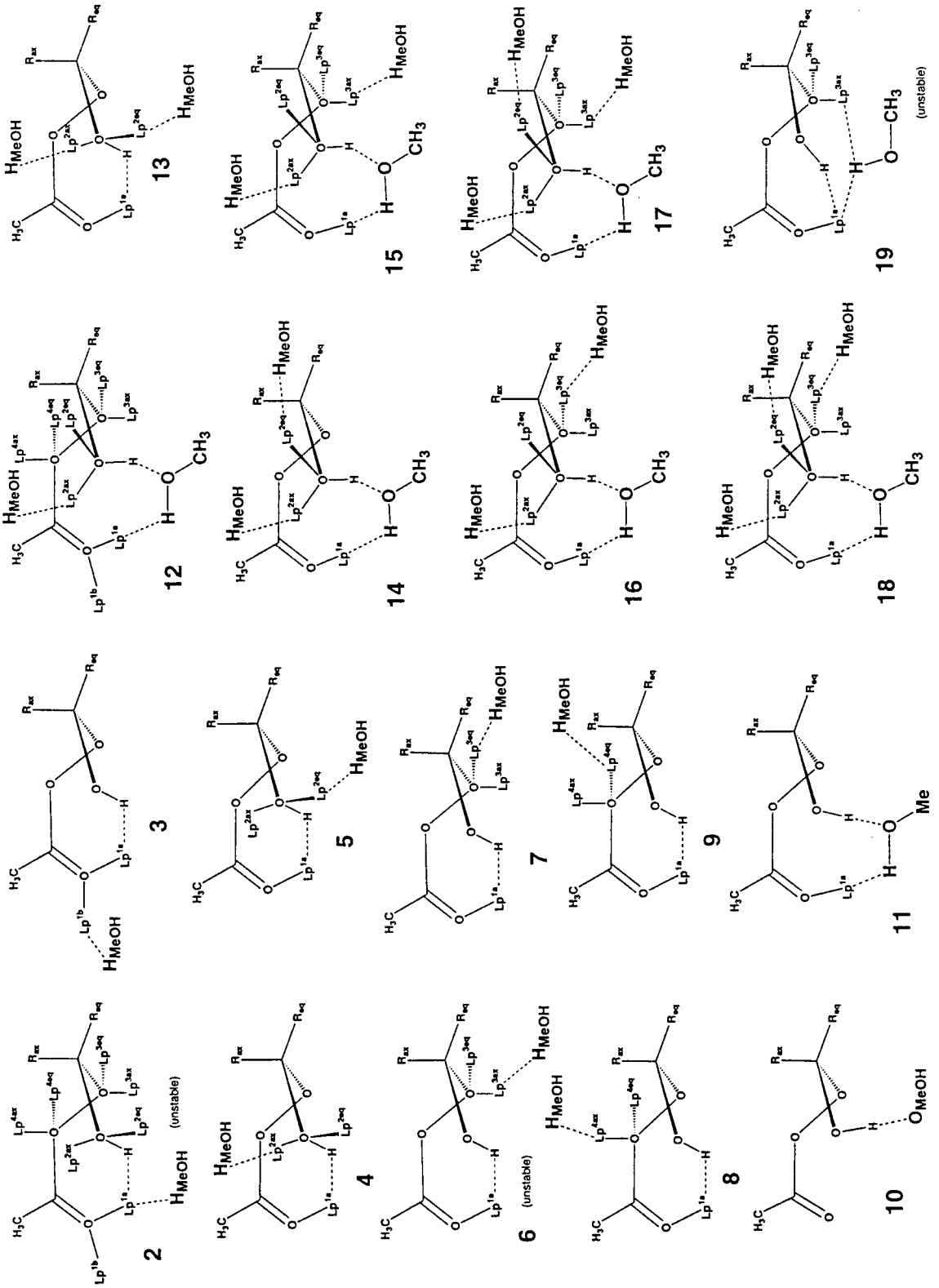

Figure 1. Epimeric adducts **2a**–**19a** and **2b**–**19b**, of which the free electron pairs of four oxygen atoms of the parent adduct **1** are indicated with notation 'Lp'. Notations 'ax' and 'eq' refer to axial and equatorial positions of the groups, respectively.

route (Table 2, entries 41–43), besides this the reactivity of pentanal was poorer than of α-branched 2-ethylhexanal or 2-ethylbutanal. Results are similar to those reported earlier.[6]

2.1. Computational studies—methods and models

In an effort to rationalise the observed solvent effects, and specifically the high conversions to acid in the case of aliphatic alcohols, calculations were carried out with models for adduct **1** using methanol as probe. The computational studies were carried out employing DFT methods at the DNPP level with the Spartan[11] program. All structures were fully optimized employing the standard options of the program. Despite the industrial importance of the process of oxidation of aldehydes to carboxylic acids, no previous computational studies on these methanol adducts of **1** appeared to be published in the literature. The utility that DFT based methods offer for inspection of compounds containing O–O bonds has been recently illustrated by Freccero, Gandolfi, Sarzi-Amade and Rastelli.[12]

Two epimers **1a** and **1b** of the parent compound of **1** (Scheme 1, R^1, R^2=CH_3) were used as models of the pseudo 7-membered ring system of **1** and methanol as a model of alcohols. Using a methanol molecule as a probe model structures **2a**–**11a** and **2b**–**11b** (Fig. 1) of alcohol-**1** adducts were generated. In these models H_{OH} of methanol interacts with the lone pairs on **1a** and **1b**.

Thus, H_{OH} of methanol interacts (Fig. 1) in **2a**–**3a** and **2b**–**3b** with the lone pairs of $O_{C=O}$; in **4a**–**5a** and **4b**–**5b** with the lone pairs of the oxygen atom of OH of the hemiacetal moiety; in **6a**–**7a** and **6b**–**7b** with the lone pairs of the oxygen of the peracid moiety adjacent to the carbon of the hemiacetal moiety; and in **8a**–**9a** and **8b**–**9b** with the lone pairs of the sp^3-hybridised oxygen adjacent to $C_{C=O}$. With the aid of these models the Lewis basicity of all of the lone pairs of **1a** and **1b** was estimated. In the case of structures **10a**–**11a** and **10b**–**11b** O_{MeOH} interacts with the OH group of **1a** and **1b**. These models were used to estimate the Lewis acidity of the hydrogen of the H_{OH} of **1a** and **1b**. A comparison of the optimized structures and relative stabilities of these adducts revealed that the most advantageous interactions of methanol with **1** occur in models **4** and **11** (Table 3).

Then, a further study on solvent effects in which one (**12a**–**13a** and **12b**–**13b**, Fig. 1), two (**14a**–**16a** and **14b**–**16b**) and finally three (**17a**–**18a** and **17b**–**18b**) additional methanol molecules were allowed to form hydrogen bonds with **4** and **11** was conducted. In these 1:2, 1:3 and 1:4 adducts the interaction sites on **4** and **11** were chosen on the basis of the relative strengths of the

Table 3. Energies (**E**) and lengths (**r**)[a] of selected bonds of **1a**, **1b** and methanol adducts **2a–19a** and **2b**–**19b** [**1**·(MeOH)$_n$; n=1–4][b]

Structure[b]	−**E** [a.u.]	**r**[a] (C=O)	**r**[a]($O_{C=O}$–H_{OH})	**r**[a](O–H)	**r**[a](O_{OH}–$C_{ald.}$)	**r**[a]($C_{Ald.}$–O_{OO})	**r**[a](O–O)	**r**[a](O_{OO}–$C_{C=O}$)
1a	454.70491	1.209	1.864	0.990	1.380	1.415	1.446	1.353
1b	454.70589	1.209	1.852	0.990	1.379	1.415	1.457	1.352
11a	569.57991	1.215	2.895	1.021	1.363	1.444	1.441	1.339
11b	569.57954	1.215	2.938	1.022	1.360	1.442	1.451	1.337
10a	569.56857	1.204	3.178	1.006	1.369	1.432	1.436	1.353
10b	569.56686	1.204	3.063	1.005	1.366	1.433	1.442	1.352
3a	569.55756	1.212	2.045	0.985	1.380	1.417	1.448	1.348
3b	569.55802	1.212	2.039	0.984	1.378	1.417	1.455	1.345
5a	569.56180	1.210	1.791	0.996	1.397	1.405	1.452	1.352
5b	569.56478	1.212	1.720	1.000	1.393	1.405	1.462	1.348
4a	569.56908	1.213	1.770	1.001	1.400	1.405	1.448	1.356
4b	569.57079	1.213	1.745	1.002	1.399	1.406	1.458	1.353
7a	569.55910	1.205	1.998	0.985	1.376	1.432	1.446	1.361
7b	569.55988	1.206	1.939	0.987	1.373	1.434	1.453	1.358
9a	569.55571	1.203	2.020	0.985	1.380	1.416	1.446	1.369
9b	569.55672	1.204	1.968	0.986	1.379	1.420	1.456	1.365
8a	569.55683	1.202	2.067	0.985	1.382	1.421	1.445	1.368
8b	569.55794	1.204	1.927	0.987	1.377	1.418	1.459	1.363
12a	684.44867	1.219	2.876	1.039	1.385	1.427	1.445	1.346
12b	684.44775	1.218	2.891	1.039	1.379	1.427	1.453	1.340
13a	684.42483	1.215	1.675	1.012	1.411	1.399	1.451	1.345
13b	684.42744	1.216	1.637	1.014	1.407	1.401	1.457	1.351
14a	799.30569	1.218	2.912	1.053	1.398	1.418	1.446	1.348
14b	799.30755	1.219	2.879	1.057	1.398	1.418	1.450	1.346
16a	799.30562	1.218	2.860	1.040	1.379	1.440	1.443	1.356
16b	799.30470	1.217	2.874	1.045	1.374	1.443	1.453	1.352
15a	799.30471	1.215	2.833	1.042	1.377	1.436	1.440	1.358
15b	799.30387	1.215	2.838	1.042	1.375	1.436	1.446	1.358
18a	914.16108	1.217	2.888	1.059	1.390	1.431	1.444	1.356
18b	914.16145	1.218	2.871	1.066	1.389	1.433	1.451	1.353
17a	914.16015	1.214	2.790	1.057	1.390	1.427	1.443	1.369
17b	914.16084	1.214	2.780	1.062	1.389	1.427	1.450	1.359
MeOH	114.84264	–	–	0.971	1.405	–	–	–
(MeOH)$_2$	229.69782	–	1.702	0.987[c]	1.397[d]	–	–	–

[a] Bond lengths (**r**) in angstroms.
[b] Fig. 1; Adducts **2**, **6** and **19** were found unstable (they all were converted to adduct **11** during the geometry optimization).
[c] The length of the O–H bond of the non-coordinating hydrogen was 0.969 Å.
[d] The length of the C–O bond of the methanol moiety donating the lone pair involved in the hydrogen bond was 1.417 Å.

interactions found in the 1:1 adducts (Table 3), as the most significant lone pairs of oxygen atoms of **1a** and **1b** for the formation of hydrogen bonds with methanol were observed to be Lp^{1a}, Lp^{2ax}, Lp^{2eq} (Fig. 1).

In order to compare the further stabilization of 1:1 adducts **4** (7-membered pseudo cyclic), **13a** and **13b** (Fig. 1) were generated by adding one molecule of methanol to **4a** and **4b**. In order to see how does the pseudo cyclic system of **11** interact with one methanol, models **12a** and **12b**, were constructed. Then models **14a**–**16a** and **14b**–**16b** were derived from **12** by adding one methanol to **12a** and **12b**. Finally, because the formation of **14** was found to be more favoring than that of **15** or **16**, the 1:4 adducts (i.e. **17a**–**18a** and **17b**–**18b**) were generated by adding one methanol to **14a** and **14b**.

By this method we first find the most important interactions between **1a**–**1b** and one methanol (1:1 adducts) and thereafter determine further stabilization of the most stable 1:1 adducts. Then we allow the most stable of the 1:1 adducts to interact with additional methanol molecules. The aim of this method is to direct the study onto the most stabilizing interactions among numerous plausible interactions of **1** and bulk alcohol. Adduct **19** was used to determine a plausible chelating interaction between H_{MeOH} and two lone pairs (L^{1a} and L^{3ax}).

In the case of methanol molecules bound only via one hydrogen bond to a lone pair on **1a** or **1b**, the initial position of the methanol (i.e. position to start the geometry optimization process) was set so that the methyl group would be directed away from the skeleton of **1a** or **1b** (i.e. the methyl group would point away from the polar atoms of **1a** or **1b** and the lone pairs of the oxygen adjacent to the methyl group would point towards the polar core of **1a** or **1b**). Optimization of the models generated in this manner gave the results (Table 3) discussed in this report.

No attempts were made to determine all possible conformations of the methanol molecules coordinated to **1a** and **1b** because that would be an exhaustive task and clearly beyond the scope of this study. Furthermore, energy differences of such conformers should be rather small and would not be necessary for the conclusions of this study. A total of 36 different methanol adducts **1**·$(MeOH)_n$ (i.e. structures **2a**–**19a** and **2b**–**19b**, Fig. 1) were studied computationally. As an internal reference the energy of formation and the length of hydrogen bond of a methanol dimer were determined (Table 3).

2.2. Computational studies—results and discussion

The total energies and bond lengths of the 7- and 9-membered pseudo cyclic systems of the optimized structures are presented in Table 3 whereas lengths of the hydrogen bonds are summarized in Table 4 (1:1 adducts) and Table 5 (1:2, 1:3 and 1:4 adducts). Chosen bond and torsion angles are shown in Table 6. Estimates of the energies of formation of the adducts are shown in Table 7.

Hydrogen bonds: Results summarized in Tables 4 and 5 indicate that both **1a** and **1b** form hydrogen bonded adducts with methanol. The tightest hydrogen bonds among the 1:1 adducts, in which methanol is not incorporated into the pseudo cyclic ring, [i.e. adducts **2**–**9**, in which there is only one hydrogen bond between methanol and **1a** or **1b**], are found in **4a** and **4b** (1.688 and 1.701 Å, Table 5), and in **5a** and **5b** (1.767 and 1.736 Å, Table 5). This indicates that Lp^{2ax} and Lp^{2eq} are the most basic of the lone pairs on **1**. The lone pair Lp^{2ax} appears to be more basic than Lp^{2eq}, because the hydrogen bonds between H_{MeOH} and $O(Lp^{2ax})$ are shorter in both **4a** and **4b** than the related bonds of $O(Lp^{2eq})$ in both **5a** and **5b**. The same conclusion can be drawn when E_F

Table 4. Lengths of hydrogen bonds of 1:1 adducts of methanol and **1**[a]

Structure[a]	Hydrogen bonds (Å)	(a)[b]	(b)[c]
1	$O(Lp^{1a})$–H_{OH}	1.897	1.839
3	$O(Lp^{1b})$–H_{Me}	1.823	1.819
4	$O(Lp^{2ax})$–H_{Me}	1.688	1.701
5	$O(Lp^{2eq})$–H_{Me}	1.767	1.736
7	$O(Lp^{3eq})$–H_{Me}	1.908	1.794
8	$O(Lp^{4ax})$–H_{Me}	1.871	1.811
9	$O(Lp^{4eq})$–H_{Me}	1.861	1.975
10	H_{OH}–$O(Lp_{Me})$	1.627	1.607

[a] Fig. 1, Adducts **2** and **6** were unstable (Table 3); Me in subscript style indicates an atom of a methanol molecule.
[b] Epimer **a**: methyl in equatorial position.
[c] Epimer **b**: methyl in axial position.

Table 5. Lengths of hydrogen bonds of nine-membered pseudo chelate **11** and its adducts to one (**12**), two (**14**–**16**) and three (**17**–**18**) methanol molecules[a]

Structure[a]	Hydrogen bonds (Å)													
	O_{Me}–H_{OH}		$O(Lp^{1a})$–H_{Me}		$O(Lp^{2ax})$–H_{Me}		$O(Lp^{2eq})$–H_{Me}		$O(Lp^{3ax})$–H_{Me}		$O(Lp^{3eq})$–H_{Me}		$(O–H)_{Me}$[b]	
	(a)[c]	(b)[d]	(a)[c]	(b)[d]	(a)[c]	(b)[d]	(a)[c]	(b)[d]	(a)[c]	(b)[d]	(a)[c]	(b)[d]	(a)[c]	(b)[d]
11	1.573	1.560	1.628	1.631	–	–	–	–	–	–	–	–	1.004	1.003
12	1.520	1.500	1.586	1.591	1.623	1.668	–	–	–	–	–	–	1.014	1.010
13	–	–	–	–	1.754	1.779	1.758	1.741	–	–	–	–	–	–
14	1.473	1.451	1.586	1.572	1.691	1.689	1.744	1.744	–	–	–	–	1.015	1.016
15	1.496	1.481	1.616	1.656	1.662	1.658	–	–	1.830	1.856	–	–	1.012	1.009
16	1.519	1.488	1.618	1.604	1.630	1.648	–	–	–	–	1.819	1.787	1.011	1.012
17	1.455	1.426	1.619	1.623	1.700	1.704	1.747	1.729	1.944	1.936	–	–	1.013	1.014
18	1.450	1.424	1.585	1.575	1.682	1.686	1.727	1.746	–	–	1.807	1.808	1.015	1.017

[a] Fig. 1, Me in subscript style indicates an atom of a methanol molecule. Adduct **19** was unstable (Table 3).
[b] The O–H bond of the bridging methanol.
[c] Epimer **a**: methyl in equatorial position.
[d] Epimer **b**: methyl in axial position.

Table 6. Selected bond (σ) and torsion (γ) angles[a] of the 7- and 9-membered pseudo-rings of the optimized structures of **1–18**[b]

Structure	σ^{a} (Me–$C_{Ald.}$–O_{OO})	σ^{a} (H–O_{OH}–$C_{Ald.}$–H)	$\gamma^{a,b}$ (Me–$C_{Ald.}$–O–O)	Structure	σ^{a} (H–$C_{Ald.}$–O_{OO})	σ^{a} (H–O_{OH}–$C_{Ald.}$–Me)	$\gamma^{a,b}$ (H–$C_{Ald.}$–O–O)
1a	101.9	−148.2	177.5	**1b**	97.3	−151.5	178.5
11a	102.1	−177.3	−171.2	**11b**	96.5	178.6	−172.9
10a	102.5	−169.6	−172.0	**10b**	97.5	−166.9	176.9
3a	102.5	157.1	−176.0	**3b**	97.4	161.4	−178.7
5a	103.3	137.9	−172.5	**5b**	97.5	144.4	−177.8
4a	103.9	141.8	−175.3	**4b**	98.9	143.1	−174.6
7a	102.7	158.2	−177.2	**7b**	97.0	160.0	178.9
9a	102.7	154.8	−175.0	**9b**	97.3	158.4	−178.9
12a	102.4	173.2	−166.5	**12b**	97.3	177.1	−168.4
13a	104.3	133.7	−171.8	**13b**	98.6	142.0	−177.3
14a	103.9	171.1	−166.0	**14b**	98.1	177.1	−168.5
16a	102.9	172.7	−164.4	**16a**	97.5	177.6	−167.2
15a	102.7	174.6	−168.0	**15b**	97.3	178.9	170.2
18a	102.9	173.2	−166.9	**18b**	97.4	177.0	−168.2
17a	103.8	172.2	−165.6	**17b**	98.0	179.4	−170.7

[a] Angles in degrees.
[b] Adducts **2**, **6** and **19** were unstable (Table 3).

Table 7. Energies of formation (E_F),[a] energies of formation (E_{CF}) corrected with the dissociation energy of methanol dimer,[b] energies of formation (E_{RF}) relative to the number of methanol molecules,[c] and energies of formation (E_{BF}) relative to the number of hydrogen bonds[d] of adducts **2–19**[e]

Structure[e]	(E_F)[a]	(E_{CF})[b]	(E_{RF})[c]	(E_{BF})[d]	Structure[e]	(E_F)[a]	(E_{CF})[b]	(E_{RF})[c]	(E_{BF})[d]
3a	−26.3	+6.8	−26.3	−13.2	**3b**	−24.9	+8.0	−24.9	−12.5
4a	−56.5	−23.6	−56.5	−28.3	**4b**	−58.5	−25.6	−58.5	−29.3
5a	−37.4	−4.5	−37.4	−18.7	**5b**	−42.7	−9.8	−42.7	−21.4
7a	−30.3	+2.8	−30.3	−15.2	**7b**	−29.8	+3.1	−29.8	−14.9
8a	−24.4	+8.7	−24.4	−12.2	**8b**	−24.7	+8.2	−24.7	−12.4
9a	−21.4	+11.5	−21.4	−10.7	**9b**	−21.5	+11.4	−21.5	−10.8
10a	−55.2	−22.3	−55.2	−55.2	**10b**	−48.1	−15.2	−48.1	−48.1
11a	−85.0	−52.1	−85.0	−42.5	**11b**	−81.4	−48.5	−81.4	−40.7
12a	−153.3	−87.7	−76.8	−51.1	**12b**	−151.2	−85.4	−75.6	−50.4
13a	−91.0	−25.4	−45.5	−30.3	**13b**	−95.2	−29.4	−47.6	−31.7
14a	−191.3	−92.9	−63.8	−47.8	**14b**	−193.6	−94.9	−64.5	−48.4
15a	−188.8	−90.4	−62.9	−47.2	**15b**	−184.0	−85,3	−61.3	−46.0
16a	−191.1	−92.7	−63.7	−47.8	**16b**	−186.2	−87.5	−62.1	−46.6
17a	−222.4	−91.2	−55.6	−44.5	**17b**	−221.6	−90.0	−55.4	−44.3
18a	−224.8	−93.6	−56.2	−45.0	**18b**	−223.2	−91.6	−55.8	−44.6

[a] Relative to starting materials.
[b] $E_{CF}=E_F-n\cdot(E_D)$, where n is the number of methanol molecules incorporated in the adduct and E_D is the dissociation energy (−32.9 kJ mol^{-1}) of the methanol dimer (Table 3).
[c] $E_{RF}=E_F/n$, where n is the number of methanol molecules incorporated in the adduct.
[d] $E_{BF}=E_F/m$, where m is the number of hydrogen bonds in the adduct (as a hydrogen bond was considered a O–H bond of which the length was in the range 1.4–2.1 Å).
[e] Epimers **a** and **b**, see Fig. 1. Adducts **2**, **6** and **19** were unstable (Table 3).

values (Table 7) of **4** and **5** are compared. The energies of formation of two epimers of **4** (−56.5 and −58.5 kJ mol^{-1}) are clearly more negative than those of the related epimers of **5** (−37.4 and −42.7 kJ mol^{-1}).

The lone pairs Lp^{2ax} and Lp^{2eq} also appear to have a role in the stabilization of the 7-membered pseudo cyclic system of **1**. A comparison of the lengths of the intramolecular hydrogen bonds of adducts **3–9** and **13** (Table 3) indicates that the bond strengthens when H_{MeOH} interacts with either one (**4** or **5**) or with both (adduct **13**) of the lone pairs Lp^{2ax} and Lp^{2eq}. In the case of **4** and **5** the values in the range of 1.720–1.791 Å indicate that H_{MeOH} interacting with Lp^{2ax} is enhancing the acidity of the hydrogen of the intramolecular hydrogen bond more than that interacting with Lp^{2eq}.

Interestingly, when the E_F values (Table 7) of **4** and **5** are compared, it can be seen that the energy of formation of **4b** (−58.5 kJ mol^{-1}) is more negative than that of **4a** (−56.5 kJ mol^{-1}). Furthermore, when the lengths of the intramolecular hydrogen bonds (Table 3) are compared we see that the bond of **4b** (1.745 Å) is shorter than that of **4a** (1.770 Å) indicating that when there is an alkyl group in the axial position (i.e. epimers **b**, R_{ax}=alkyl; R_{eq}=H, Fig. 1) the intramolecular hydrogen bond is tighter than in the case of R_{ax}=H (epimers **a**). This result is interesting because the shorter the intramolecular hydrogen bond of **1** the more closely the structure should resemble (on the basis of Hammond's postulate) the transition state of the reaction. Therefore, the shorter intramolecular hydrogen bond, the more easily it should undergo the rearrangement reaction (Scheme 1). The results discussed above indicate that in adducts **b** the intramolecular hydrogen bond is shorter (than in adducts **a**) and therefore pathway **a** (Scheme 1) should be favored over **b** in the presence of methanol. This is consistent with the experimental observations.

The length of intramolecular hydrogen bond (Table 3) of **5b** (1.720 Å) is clearly shorter than that of **5a** (1.791 Å) and the energy of formation (Table 7) of **5b** (−42.7 kJ mol^{-1}) is more negative than that of **5a** (−37.4 kJ mol^{-1}). In the case of **13b** and **13a** the corresponding bond lengths are 1.637 Å and 1.675 Å and the energies −95.2 and −91.0 kJ mol^{-1}, respectively. Therefore, as in the case of **5** and **13** the lengths of the intramolecular hydrogen bonds of epimers **b** (i.e. R_{ax}=CH_3; R_{eq}=H, Fig. 1) are clearly shorter and the energies of formation more negative than the related values of epimers **a** (i.e. R_{ax}=H; R_{eq}=CH_3), we could conclude, that when a proton of a protic solvent interacts with the lone pairs Lp^{2ax} and Lp^{2eq} of **1**, adducts in which the hydrogen of the hemiacetal group is in an equatorial position (i.e. R_{eq}=H, Fig. 1) would have a more advantageous geometry for the rearrangement reaction to occur (along pathway **a**, Scheme 1) than their epimers (along pathway **b**). As described above in the case of **4a/4b**, this is consistent with the experimental observations.

The conclusion related to the favor of pathway **a** (Scheme 1) drawn above on the basis of the 1:1 methanol adducts to **1a** and **1b** can also be drawn by inspecting the lengths of hydrogen bonds of methanol-bridged adducts **11–12** and **14–18** in the light of the mechanism depicted in Scheme 2 and Hammond's postulate. A comparison of the shortening (**S**, Scheme 2) and lengthening (**L**, Scheme 2) bonds of epimers (**a** and **b**) of adducts **11–12** and **14–18** (Fig. 1, Tables 3 and 5) gave rise to the following conclusions: (1) **L1** is longer (or equally long) in **b** than in the corresponding epimer **a** [except in **12**; Table 3, (C=O)]; (2) **S1** is shorter in **b** than in **a** [except in **11**, **12**, **15** and **17**; Table 5, ($O_{C=O}$–H_{MeOH})]; (3) **L2** is longer in **b** than in **a** [except in **12** and **15**; Table 5, $(O–H)_{MeOH}$]; (4) **S2** is shorter in **b** than in **a** [Table 5, (O_{MeOH}–H_{OH})]; (5) **L3** is longer (or equally long) in **b** than in **a** [Table 5, (O–H)]; (6) **S3** is shorter (or equally long) in **b** than in **a** [Table 3, (O_{OH}–$C_{ald.}$)]; (7) **L4** is longer in **b** than in **a** [Table 3, (O–O)]; (8) **S4** is shorter (or equally long) in **b** than in **a** [Table 3,

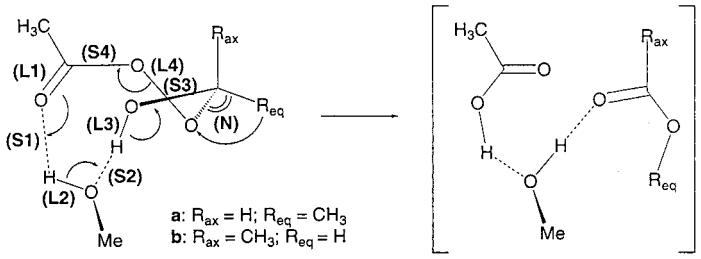

Scheme 2. Changes of bonding in the transition state of the rearrangement of methanol-stabilized aldehyde–peracid adduct **11** involving the migration of R_{eq} group. Shortening of bonds is indicated with notation '**S**' whereas lengthening of bonds is indicated with '**L**'. The angle that the migrating group forms with the bond along which the migration occurs is indicated with '**N**'.

(O_{OO}–$C_{C=O}$)]; (9) **N** is narrower (the narrower the bond angle, the more closely the structure resembles the transition state of the migration of R_{eq}) in **b** than in **a** [Table 6, σ(H–$C_{Ald.}$–O_{OO})>σ(Me–$C_{Ald.}$–O_{OO}) for all adducts]; and, (10) γ(R_{eq}–$C_{Ald.}$–O–O) (Table 6) is closer to 180.0° in **b** (R_{eq}=H) than in **a** (R_{eq}=Me; the closer the torsion angle is to 180.0°, the easier the migration of R_{eq} would be, because the leaving and migrating groups should be *trans* about the O–C bond, along which the migration takes place).

Interestingly, all these ten comparisons of structural features of methanol-bridged adducts **11**–**12** and **14**–**18** suggest that the structures of epimers **b** resemble the transition state of the reaction (Scheme 2) more closely than structures of the corresponding epimers **a** do. Furthermore, conclusions similar to those discussed above can also be drawn in the case of 1:1 adducts **3**–**5**, **7**–**10** and **13** for the changes **L1** [Table 3, (C=O)], **S2** (in the case of **10**, Table 4), **L3** [except in **3** and **10**, Table 3, (O–H)], **S3** [Table 3, (O_{OH}–$C_{ald.}$)], **L4** [Table 3, (O–O)], **S4** [except in **13**, Table 3, (O_{OO}–$C_{C=O}$)], **N** [Table 6, σ(H–$C_{Ald.}$–O_{OO}) and σ(Me–$C_{Ald.}$–O_{OO})], and γ(R_{eq}–$C_{Ald.}$–O–O) (except in **4**, Table 6). Therefore, as in the case of epimers **b**, the migrating group is hydrogen (i.e. R_{eq}=H, Fig. 1, Scheme 2), the result of this comparison is, in the light of Hammond's postulate, consistent with the experimental observation that in the presence of alcohol the rate of formation of acid is enhanced.

Performance of the models: The estimated energies of formation (E_F) of adducts **2**–**18** shown in Table 7 indicate that addition of methanol molecules to **1a** and **1b** to form hydrogen bonded systems is energetically favored in the gas phase (E_F values continuously decrease with the increasing molar ratio of methanol in the adducts). If we try to estimate what could happen in methanol solution, we need to take into account the structure of liquid methanol.

The minimum requirement for estimating the difference of energetics of gas phase and liquid phase reactions would be to consider the energy that is needed for the separation of a methanol molecule from bulk methanol. For the purposes of this study, a rough estimate of this energy was provided by the energy of dissociation of a methanol dimer $(MeOH)_2$ (-32.9 kJ mol^{-1}, calculated on the basis of the values shown in Table 3). Namely, although the real value of separating a methanol molecule from bulk methanol would be much larger, this method of estimation is reasonable, because when we release a methanol molecule from the dimer we break one hydrogen bond. When the methanol molecule coordinates to **1** or to methanol-bridged adducts of **1** we create one hydrogen bond (except in the case of the formation of **11**). In this way, errors emanating from the computational method used should be minimized allowing comparisons of relative values (instead of absolute ones). For example, the energies (E_{CF}, Table 7) corrected using the dissociation energy of methanol dimer indicate that the energy of formation of the adducts **1a**·$(MeOH)_n$ and **1b**·$(MeOH)_n$ decreases until the level of n=2 (e.g. E_{CF} of **12a** and **12b** are -87.7 and -85.4 kJ mol^{-1}, Table 7).

Adding more methanol decreases the energy only in small amounts [e.g. adding one methanol to **12a** gives **14a** ($E_{CF}=-92.9$ kJ mol^{-1}) and further adding one more methanol to **14a** gives **18a** ($E_{CF}=-93.6$ kJ mol^{-1}) indicating saturation]. The saturation phenomenon discussed above can be seen also if the energies of **2**–**18** are calculated per methanol molecule incorporated (E_{RF}, Table 7). The E_{RF} values of methanol-bridged adducts continuously grow when methanol is added to **11** indicating that the new methanol molecules added would stabilise the adduct less than the first one needed for the formation of the pseudo nine-membered ring system of **11**. Conclusions similar to these can be drawn also when the values of the energy of formation per the number of hydrogen bonds (E_{BF}, Table 7) or tightening of the H_{OH}–O_{MeOH} bond (Tables 4 and 5) are inspected.

When energies (E_{CF}, Table 7) of the adducts involved in the reaction sequence **1→10→11→12→14→18** were represented (for both epimers **a** and **b**) as a function of the number of hydrogen bonds in the adducts, the graphs shown in Fig. 2 (E_{CF}=E1 and E_{RF}=E2) were obtained. As expected on the basis of the discussion above, the energy E_{CF} decreases fast till the level of three hydrogen bonds and the energy E_{RF} decreases fast till the level of two hydrogen bonds (Fig. 2).

When the length of the H_{OH}–O_{MeOH} bonds (Tables 4 and 5, Fig. 3) of both **a** and **b** epimers in the sequence **1→10→11→12→14→18** were represented as a function of the number of hydrogen bonds in the adducts, the graphs shown in Fig. 3 were obtained. In this case we observe that the H_{OH}–O_{MeOH} bond of the bound methanol continuously shortens till the level of four hydrogen bonds [i.e. the change related to the addition of the fourth methanol molecule to **1a** and **1b** (i.e. to convert **14** to **18**) is smaller than the changes caused by the previous additions]. In the light of these

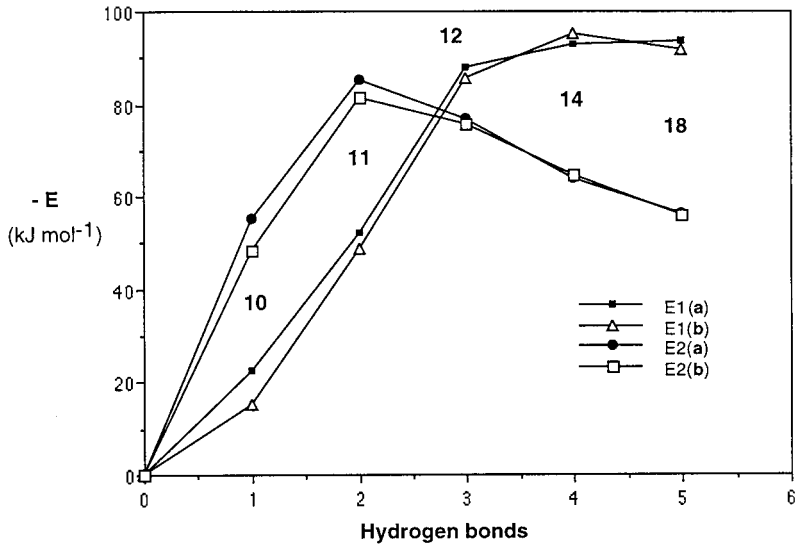

Figure 2. Energies (E1=E_{CF} and E2=E_{RF}; Table 7) of the formation of adducts **18a** and **18b** via the pathways **1a→10a→11a→12a→14a→18a** and **1b→10b→11b→12b→14b→18b** as a function of the number of hydrogen bonds.

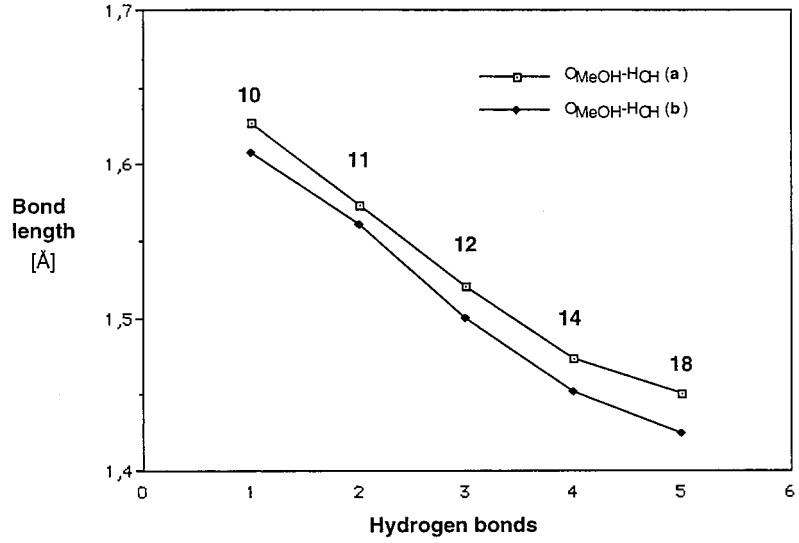

Figure 3. The length of the $(H–O)_{MeOH}$ bond of the bridging methanol in adducts formed via the pathways **1a→10a→11a→12a→14a→18a** and **1b→10b→11b→12b→14b→18b** as a function of the number of hydrogen bonds.

results we conclude that the results of the comparison of structural parameters of methanol adducts **1a**·$(MeOH)_n$ and **1b**·$(MeOH)_n$ discussed above would not have changed significantly if the number of methanol molecules bound by the parent compounds **1a** and **1b** had been larger than four.

3. Conclusions

Methanol, propanol and *i*-propanol were the best alcoholic solvents for 2-ethylhexanoic acid formation (selectivity ~93%). A phenyl group in an α-position made the aldehyde more sensitive to solvent effects than an aliphatic carbon chain. The highest selectivity, ~78%, of 2-phenylpropanal to 2-phenylpropanoic acid was afforded in *i*-propanol, in *t*-butanol selectivity for the carboxylic acid was ~55% and in benzyl alcohol only ~35%. Still, compared with toluene, in which only 5% of aldehyde reacted to acid, the difference was significant.

The highest concentration of formate was obtained in chlorinated solvents (dichloroethane, chloroform) and toluene. In added peracid oxidised reactions, the formate route of 2-ethylhexanal–peracid adduct dominated in chlorinated solvents by ~70–75% and in toluene by ~64%. 2-Phenylpropanal was almost completely oxidised to formate in both toluene and dichloromethane as well as in octanoic acid.

Computational calculations revealed that the insertion of methanol into the seven-membered hydrogen bonded pseudo ring of aldehyde–peracid adduct **1** leading to chelate **11** (a nine membered ring system containing two hydrogen bonds) is the most advantageous reaction among those of the formation of **1a**·$(MeOH)_n$ studied. The experimentally

observed formation of acid (pathway **a**, Scheme 1) in the presence of alcohol was rationalised on the basis of the computational study and Hammond's postulate: the structural similarity of adducts **b** (reacting via pathway **a**, Scheme 1) to the transition state of the reaction (Scheme 2) was higher than that of adducts **a** (reacting via pathway **b**, Scheme 1).

The computational results of this study show that methods of theoretical chemistry can be used to better understand solvent effects at the molecular level. The importance of computational inspections is enhanced in the case of reactions of labile intermediates which are difficult to study experimentally.

4. Experimental

4.1. General

2-Ethylhexanal, 2-ethylbutanal, pentanal, 2-phenylpropanal, and all the solvents were dried, distilled and preserved under inert atmosphere until use.

Gas chromatographic analyses were performed with an HP 6890 instrument: Polar Innowax column 30 m; initial column temperature 40°C final column temp. 250°C; progress rate 10°C/min; constant flow 6.3 ml/min of carrier gas; initial pressure 0.93 bar. The main oxidation products of aldehydes were identified and quantified by comparison with authentic samples. Amount of 2-formyl butanal was quantified by using 3-formyl heptanal (For preparation see below) as standard and amount of 2-phenyl propyl formate by using 2-phenylpropanoic acid as standard. Decane or tetradecane was used as internal standard to calculate the exact amount of substance present in the reaction mixture.

The oxidation products were also identified by GC-MS. The sample components were identified using gas chromatography-mass spectrometry in full scan mode with electron impact (EI) and chemical ionisation (CI). The EI spectra were identified by using the NIST-EPA-NIH Mass Spectral Library (version 1.5a) and manual interpretation. The CI spectra were used to confirm the molecular weight of unknowns in ambiguous case.

The EI spectra were measured using an HP Mass Selective detector interfaced to HP 6890 Gas chromatograph. The MS scan range was m/e 25–500 and the speed 1 scan/sec. The ion source temperature was 230°C and the quadrupole temperature 150°C. The CI spectra were measured using a VG Prospec sector mass spectrometer interfaced to an HP 5890 Series II Gas Chromatograph. The scan range was *m/e* 80–500 and scan speed 2 sec./decade. The ion source temperature was 200°C. Isobutene was used as reagent gas and the ion source pressure was maintained at 2×10^{-5} mbar by regulating the reagent gas flow. In both ionisation cases the GC columns and parameters were identical to those of simple GC analyses. The GCMS interface was kept at 280°C and the electron multiplier voltage was adjusted to obtain proper sensitivity in both cases.

4.2. Oxidation of aldehyde

A flat-bottomed glass vessel equipped with condenser and oxygen balloon was charged with aldehyde, internal standard and solvent if used. Magnetic stirring (1000–1250 rpm) was commenced and the reaction mixture was evacuated and oxygenated three times at the chosen temperature. When reactions were done in air airflow in synthesis was 34 ml/min.

4.3. Preparation of 3-heptyl formate used as model compounds

3-Heptyl formate was prepared from the corresponding alcohol (20 mmol) with dimethylformamide (20 mmol) and benzoyl chloride (20 mmol) in 12 ml dichloroethane according to method of Barluenga et al.[13] Besides formate, a small amount of unreacted 3-heptanol was present in the crude product. The formate was purified by vacuum distillation and the yield was 39%.

Acknowledgements

The TEKES foundation is acknowledged for partial financial support.

References

1. Reviews include: (a) McNesby, J.; Heller, C. *Chem. Rev.* **1954**, *54*, 325. (b) Sajus, L.; Roch, S. *Comprehensive Chemical Kinetics*, Bamford, C., Tipper, C., Eds.; Elsevier: New York, 1980; Vol. 16, pp 89.
2. For example: (a) Godfrey, I.; Sargent, M.; Elix, J. *J. Chem. Soc., Perkin Trans. 1* **1974**, 1353. (b) Royer, J.; Beuglemans-Verrier, M. C. R. *Acad. Sc. Paris, Serie C* **1971**, 1818. (c) Camps, F.; Coll, J.; Messeguer, J.; Pericas, M. *Tetrahedron Lett.* **1981**, *22*, 3895.
3. DeBoer, A.; Ellwanger, R. *J. Org. Chem.* **1974**, *39*, 77.
4. Alcaide, B.; Aly, M.; Sierra, M. *J. Org. Chem.* **1996**, *61*, 8819.
5. Barrero, A.; Alvarez-Manzaneda, E.; Alvarez-Manzaneda, R.; Chahboun, R.; Meneses, R.; Aparicio, M. *Synlett* **1999**, 713.
6. Lehtinen, C.; Nevalainen, V.; Brunow, G. *Tetrahedron* **2000**, *56*, 9375.
7. Lehtinen, C.; Brunow, G. *Organic Process & Development* **2000**, *4*, 544.
8. Yamada, T.; Takai, T.; Rhode, O.; Mukaiyama, T. *Chem. Lett.* **1991**, 5.
9. Ohakahatsu, Y.; Takeda, M.; Hara, T.; Osa, T.; Misono, A. *Bull. Chem. Soc. Jpn* **1967**, 1423.
10. Maslow, S.; Bluymberg, E. *Russ. Chem. Rev.* **1976**, *45*, 155.
11. Wavefunction Inc., 18401 Von Karman Ave., Suite 370, Irvine, CA 92612, USA.
12. Freccero, M.; Gandolfi, R.; Sarzi-Amade, M.; Rastelli, A. *J. Org. Chem.,* **1999**, *65*, 2030.
13. Barluenga, J.; Campos, P.; Gonzales-Nunéz, E.; Asensio, G. *Synth. Commun.* **1985**, 426.